Journal of Materials Chemistry A

COMMUNICATION

View Article Online
View Journal | View Issue

Cite this: J. Mater. Chem. A, 2015, 3, 22031

Received 5th August 2015
Accepted 12th October 2015

DOI: 10.1039/c5ta06108c

www.rsc.org/MaterialsA

Design of an active and durable catalyst for oxygen reduction reactions using encapsulated Cu with N-doped carbon shells (Cu@N-C) activated by CO_2 treatment†

Seung Hyo Noh,[a] Min Ho Seo,[b] Xiao Ye,[a] Yuki Makinose,[c] Takeyoshi Okajima,[a] Nobuhiro Matsushita,[c] Byungchan Han*[d] and Takeo Ohsaka*[a]

Cu@N-C with the Cu particles encapsulated in N-doped carbon shells, which was activated by CO_2 treatment, is an excellent electrocatalyst for the oxygen reduction reaction (ORR) with a high activity and durability.

Oxygen reduction is one of the key chemical reactions that power various renewable energy devices such as polymer electrolyte membrane fuel cells (PEMFCs) and metal-air batteries. In practice, the oxygen reduction reactions (ORRs) in these applications are sluggish, limiting the overall system performance. Accordingly, conventional nano-scale Pt-based catalysts are used to reduce the activation energy for ORRs.[1,2] However, the high material cost and electrochemical instability[3,4] have resulted in delays for a wide range of commercial applications of renewable energy systems.

To date, numerous non-precious metallic or metal-free catalysts have been demonstrated to be alternatives to the traditional Pt catalysts. For example, the ORR activities of macrocyclic metal complexes[5–8] and metal oxides[9] such as iron phthalocyanine (FePc), polyaniline–iron–carbon (PANI–Fe–C),[10] Co_3O_4,[11] and $MnCo_2O_4$ (ref. 12) were often reported to be comparable to those of Pt. However, the performances of these catalysts were only approved in laboratory-scale tests and not successfully used in actual devices for long-term operations largely because of physical or electrochemical instabilities.

Recently, Fe-based materials[13] were reported to enable the manifestation of improved ORR activity and long-term electrochemical stability against dissolution in acidic or alkaline media[14] and oxidation by air if they were entirely encapsulated in carbon shells. These studies introduced new methods to overcome the conventional limits of catalysts (*i.e.*, activity and stability) for metal-air batteries,[15] PEMFCs,[13] and biological[16] and magnetic[17] materials. State-of-the-art ORR catalysts encapsulating non-precious transition metals with N-doped carbon shells were studied by several groups using transition metals such as (Fe@N-C or Fe_3C@N-C[18]) and FeCo[19,20] or NiCo[21] alloys. In the literature, it was observed that the noble structures dramatically improved ORR activity compared with typical non-precious catalysts and certain interactions between inner metals and carbon shells were conjectured as the underlying reason.

A previous work[22] showed that N-doped graphene on a Cu support (N-Gr/Cu) could be a promising ORR catalyst that performs as well as the Pt(111) surface[2] but only when the Cu is protected against surface segregation or oxidation by oxygen or water. In this study, we dramatically improved the thermodynamic and electrochemical stability of Cu particles by completely surrounding them with spherical shaped N-doped carbons (Cu@N-C). Furthermore, we rationally designed the thickness of the carbon shells using a CO_2 treatment at high temperature to control the atomistic interactions between the encapsulated Cu and the N-C shell while protecting Cu from agglomeration and electrochemical dissolution.

Using first-principles density functional theory (DFT) calculations and experimental materialization, we accurately characterized and validated the ORR activity and long-term durability of the Cu@N-C catalyst.

The Cu@N-C catalyst was synthesized *via* sustainable precursors, such as sucrose and ammonium sulfate, which are utilized as table sugar and fertilizer, respectively. Moreover, Cu metal encapsulated in carbon is relatively an abundant material

[a]Department of Electronic Chemistry, Interdisciplinary Graduate School of Science and Engineering, Tokyo Institute of Technology, 4259-G1-5 Nagatsuta, Midori-ku, Yokohama, 226-8502, Japan. E-mail: ohsaka.t.aa@m.titech.ac.jp; Fax: +81-45-924-5489; Tel: +81-45-924-5404

[b]Department of Chemical Engineering, Waterloo Institute for Nanotechnology, Waterloo Institute of Sustainable Energy, University of Waterloo, 200 University Ave. W, Waterloo, ON, N2L 3G1, Canada

[c]Materials and Structures Laboratory, Tokyo Institute of Technology, 4259 Nagatsuta, Midori, Yokohama, Kanagawa 226-8503, Japan

[d]Department of Chemical and Biomolecular Engineering, Yonsei University, Seoul, 120-749, Republic of Korea. E-mail: bchan@yonsei.ac.kr; Fax: +82-2-321-6401; Tel: +82-2-2123-5759

† Electronic supplementary information (ESI) available: Experimental detail, computational detail, and additional figures mentioned in this article. See DOI: 10.1039/c5ta06108c

compared to the Pt catalyst. The Cu@N-C catalyst was fabricated according to the described procedures in the Experimental section and Fig. S1 in the ESI.† We synthesized three different types of catalysts with various applied processes: (i) hydrothermally treated "Cu@N-C(hydro)", (ii) "Cu@N-C(heat)", which was heat-treated at $T = 1000$ °C for 2 h, and (iii) "Cu@N-C(CO_2)", which was oxidized by CO_2 for 15 min at $T = 1000$ °C. CO_2 (ref. 23) and O_2 (or air)[24] were previously used to oxidize carbon shells at high temperature. For example, Chen *et al.* used CO_2 gas to eliminate the carbon shells in Fe@C nanoparticles and obtained pure carbon nanotubes after removing Fe through an acidic treatment. We applied the CO_2 treatment to regulate the carbon shell thickness *via* oxidation reactions at high temperature. This step is a key process in controlling the electronic interactions between inner Cu particles and adsorbates from the intermediates of the ORR on the carbon shell of the Cu@N-C catalyst.

Fig. 1 shows successfully synthesized Cu@N-C(CO_2) particles. Cu@N-C particles (an average size of 450 nm) were supported on a carbon microsphere (average size: 3.4 μm) as shown in Fig. 1a, and the Cu particles were entirely encapsulated in carbon shells as shown in Fig. 1b. Using the element mapping method in Fig. 1d–g, we identified C, N, Cu, and O in Cu@N-C particles. In particular, the Cu particles are clearly distinguished from the carbon microsphere supports, and N and O atoms are well dispersed over the carbon. Defects in the carbon microspheres of Cu@N-C(CO_2) are shown in Fig. 1h and i.

There were bare Cu particles without carbon shell covers in the Cu@N-C(hydro), Cu@N-C(heat) and Cu@N-C(CO_2) catalysts, as shown in Fig. S2a–c.† The XPS spectra in Fig. 2a and b (or Fig. S5† for details) also clearly show the surface-exposed Cu particles. The X-ray diffraction patterns in Fig. 2d indicate that there was bulk fcc Cu (the sharp peaks), but no Cu oxide and Cu carbide were detected in all samples. As shown in Fig. 2c and S6,† the doping level of N in the Cu@N-C(CO_2) catalyst was approximately 1.8%, and pyrrolic *N* (50.5%) was dominant over the graphitic (19.8%) and pyridinic (29.7%) *N* structures.

To characterize the ORR activity of the Cu@N-C materials, rotating ring disk electrode (RRDE) voltammetry was applied, as shown in Fig. 3a and b. It is clearly demonstrated that Cu@N-C(hydro) and Cu@N-C(heat) are far less active than the Pt/C catalyst. We found that the Cu@N-C(heat) powder lost approximately 44 wt% of its original mass after the CO_2 treatment (Fig. S2d and e†), which implies that the carbon shells became substantially thin because of the treatment.[23]

Surprisingly, Cu@N-C(CO_2) dramatically enhanced the ORR activity to a similar level to Pt/C. Fig. 3b (Table S1 in the ESI†) shows that the onset (E_{onset}) and half-wave ($E_{1/2}$) potentials of the ORR in Cu@N-C(CO_2) are 0.94 and 0.83 V *vs.* RHE (reversible hydrogen electrode), respectively. Indeed, they were similar to those of Pt/C (1.05 and 0.85 V *vs.* RHE, respectively). In addition, the measured number of electrons (*n*) that were involved in the ORR with Cu@N-C(CO_2) was 3.95 (Fig. 3a). Thus, Cu@N-C(CO_2) enables the reduction of O_2 to H_2O with less than 3% H_2O_2 produced. The linear Koutecky–Levich plots in Fig. 3c, where the slopes are constant regardless of the electrode potential, imply that the ORR is dominated by the first-order kinetics between Cu@N-C(CO_2) and dissolved oxygen.[25]

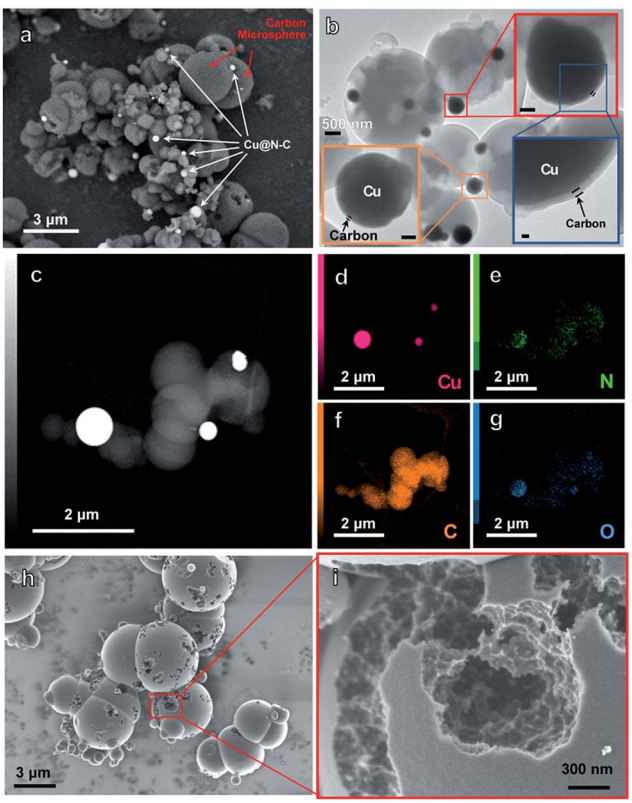

Fig. 1 (a) FE-SEM image of the Cu@N-C(CO_2) catalyst. (b) TEM images of Cu@N-C(CO_2) with three insets, which are colored with red, orange, and navy boxes and have scale bars of 100, 100 and 20 nm, respectively. (c) HAADF-STEM image of Cu@N-C(CO_2). The elemental mapping of the HADDF-STEM image indicates the existence of (d) Cu, (e) N, (f) C and (g) O. SEM images of Cu@N-C(CO_2) (h and i).

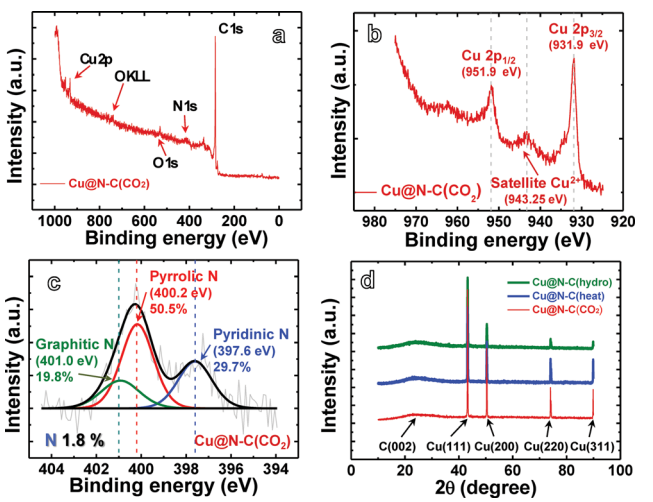

Fig. 2 (a) Overall survey spectrum, (b) Cu 2p spectrum and (c) N 1s spectrum of the Cu@N-C(CO_2) catalyst using an X-ray photoelectron spectroscope (XPS). (d) X-ray diffraction (XRD) patterns of Cu@N-C(hydro), Cu@N-C(heat) and Cu@N-C(CO_2).

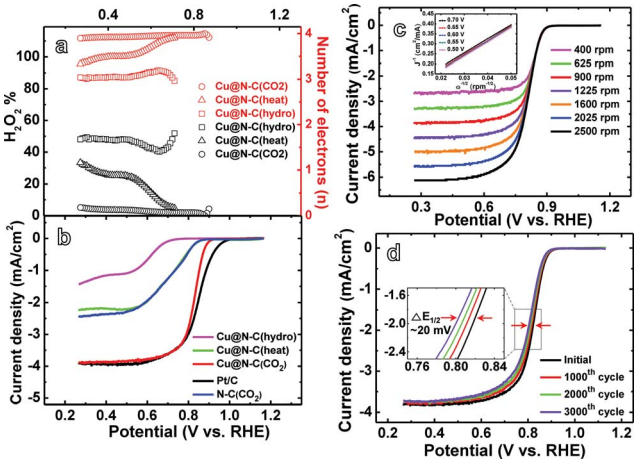

Fig. 3 ORR activity and durability of the Cu@N-C catalysts. (a) Number of electrons and H_2O_2 formation percentage. (b) Steady-state voltammograms of the ORR with Cu@N-C(hydro), Cu@N-C(heat), Cu@N-C(CO_2), N-C(CO_2) and Pt/C in O_2-saturated 0.1 M KOH solution. The scan rate and rotating speed were 5 mV s^{-1} and 900 rpm, respectively. (c) Steady-state voltammograms of the ORR with Cu@N-C(CO_2) at various rotating speeds and Koutecky–Levich plots at various electrode potentials (inset and also Fig. S8†). (d) Steady-state voltammograms of the ORR during the potential cycling durability test (potential range: 0.6–1.0 V *vs.* RHE, scan rate: 50 mV s^{-1}) in O_2-saturated 0.1 M KOH.

Nevertheless, Cu@N-C(hydro) and Cu@N-C(heat) showed much lower ORR activities than Cu@N-C(CO_2), which indicates that the bare Cu particles around Cu@N-C(hydro) and Cu@N-C(heat) cannot catalyze the ORR at all. In other words, the ORR activities are mainly determined by the Cu@N-C catalysts and not by the bare Cu around them. As shown in Fig. 1h and i, Cu@N-C(CO_2) includes the defects of the carbon microsphere, whereas Cu@N-C(heat) does not, as shown in Fig. S3g.† To understand the effect of defects on the ORR, N-doped carbon microspheres that were treated with CO_2 (N-C(CO_2)) were fabricated,[26] and the synthesis processes were identical to that of Cu@N-C(CO_2) except for the absence of the Cu precursor. The measured ORR activity (E_{onset} = 0.87 V and $E_{1/2}$ = 0.71 V) of N-C(CO_2) was much worse than that of the Cu@N-C(CO_2) catalyst as shown in Fig. 3b, which implies that the encapsulated Cu particles play a crucial role in enhancing the ORR activity.

In addition to the superior ORR activity, Cu@N-C(CO_2) exhibits outstanding electrochemical durability, as shown in Fig. 3d. In potential cycling tests between 0.6 and 1.0 V (*vs.* RHE), $E_{1/2}$ decreased by only 20 mV after 3000 cycles. The chronoamperometric current–time (*i vs. t*) responses were measured at a fixed potential of 0.7 *vs.* RHE to compare the electrochemical stability of Pt/C and Cu@N-C(CO_2) (Fig. S9†). From the beginning, the current of Pt/C steeply decreased, whereas the decrease was much milder in Cu@N-C(CO_2). Cu@N-C(CO_2) lost only 8% of the initial current value even after 30 000 s, but lost 33% in Pt/C for the identical cycling time. The excellent durability can be originated from the encapsulation of Cu particles by N-doped carbon shells, which may endow the Cu@N-C catalyst with sufficient electrochemical stability against oxidation of the core Cu in alkaline solution.

To identify the ORR active sites in the Cu@N-C catalysts, we calculated the adsorption energies of oxygen (eqn (S5)†) using density functional theory calculations (Fig. S10 and Table S2†). Fig. 4a is the model system for the Cu@N-C catalysts, and the structure is assumed as the copper particle covered by one layer N-doped carbon. We assumed a N doping level of 2.1 at% as proposed by XPS analysis (1.8%), including previous experimental[27] and theoretical[28] reports. The T_{C1} site, which is the nearest neighboring C from the doped N, strongly adsorbs O (3.82 eV), whereas the T_N site (atop of N) is the weakest adsorbing site (1.87 eV), which is consistent with previous results[22] on the bulk N-Gr/Cu system. The calculated binding energies of O on Cu@N-C and bulk Pt(111) surfaces were 3.82 and 4.44 eV, respectively, as shown in Fig. 4. According to the proposed electronic structure theory for ORR catalysts of Nørskov and his associates,[29] the Cu@N-C and Pt(111) surfaces are expected to have similar ORR activities. The obtained oxygen adsorption energies of Empty@N-C and pure Cu were 3.43 and 5.30 eV, respectively, which implies that both structures are not suitable for the ORR catalyst because they have too weak (Empty@N-C) and too strong (pure Cu) chemical bondings with O.[30]

Accordingly, N-doped carbon (N-C) shells play a key role in regulating the adsorption energy of O, which substantially enhances the ORR activity to a level comparable to the Pt(111) surface. The electronic interactions between the inner Cu particle and N-C shells can be described using an electronic charge distribution as shown in Fig. 4b. The encapsulated Cu particle clearly donates electronic charges to the N-C layers on average 0.07 e per Cu atom, which is absent in the Empty@N-C structure (Fig. S11†). Consequently, the N-C shell that encapsulates the Cu particle enables favorable electronic interactions with adsorbates in the ORR.[22] The electronic charge donation may also increase the interface contact force between the Cu

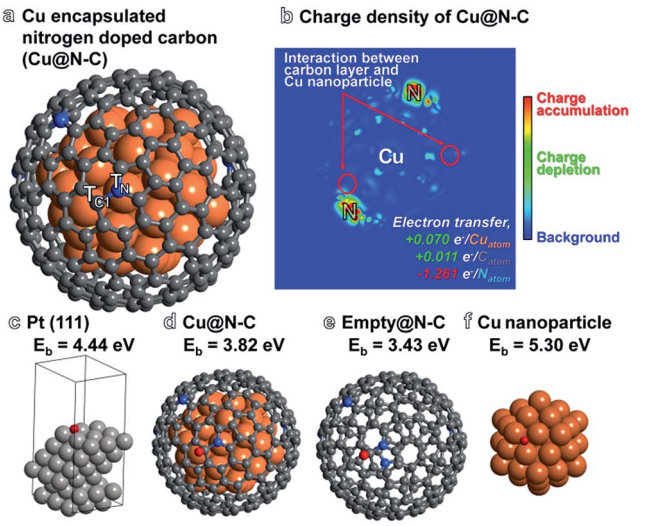

Fig. 4 Theoretical modeling of the Cu@N-C structure. (a) Model system of Cu encapsulated in nitrogen-doped carbon. (b) Charge density of Cu@N-C. Oxygen binding energies and structures of (c) Pt(111), (d) Cu@N-C, (e) Empty@N-C and (f) Cu nanoparticle.

particle and N-C shells. A detailed electronic density distribution in Cu@N-C is illustrated in Fig. S11 and S12.†

Conclusions

We synthesized Cu@N-C (CO_2), where Cu particles were completely encapsulated in N-doped carbon shells, and the shell thickness was optimized by oxidizing carbons with CO_2. Using experimental measurements and DFT calculations, we found that the catalysts have outstanding properties in both ORR activity and electrochemical durability *via* a favorably induced electronic interaction between the inner Cu and N-C shells. Furthermore, the N-C shells strongly protect the Cu particle against dissolution into aqueous solutions or chemical oxidation. Cu@N-C(CO_2) has significantly better ORR activity than the Cu@N-C particles that were fabricated using hydrothermal or only heat treatments. Our approach will be notably useful to the design of highly active, durable and cheap catalysts for a wide range of applications, *e.g.* for electrochemical devices, as promising alternatives to the costly Pt-based catalysts.

Acknowledgements

This study was supported by the Ministry of Education, Culture, Sport, Science and Technology (MEXT), Japan and the Global Frontier Program through the Global Frontier Hybrid Interface Materials (GFHIM) of the National Research Foundation of Korea (NRF), which is funded by the Ministry of Science, ICT & Future Planning (grant number 2013M3A6B1078882). The New and Renewable Energy R&D Program (20113020030020) under the Ministry of Knowledge Economy, Republic of Korea partially supported this work. This study was performed using Tsubame 2.5 at the Global Scientific Information and Computing Center of Tokyo Institute of Technology. The authors gratefully acknowledge Dr Y. Nabae for BET surface area measurements. Seunghyo Noh also thanks the Government of Japan for the MEXT scholarship.

References

1 M. Doyle, G. Rajendran, W. Vielstich, H. A. Gasteiger and A. Lamm, *Handbook of Fuel Cells Fundamentals, Technology and Applications*, Wiley, New York, 2003.
2 J. Greeley, I. Stephens, A. Bondarenko, T. P. Johansson, H. A. Hansen, T. Jaramillo, J. Rossmeisl, I. Chorkendorff and J. K. Nørskov, *Nat. Chem.*, 2009, **1**, 552–556.
3 S. H. Noh, B. Han and T. Ohsaka, *Nano Res.*, 2015, **8**, 3394–3403.
4 S. H. Noh, M. H. Seo, J. K. Seo, P. Fischer and B. Han, *Nanoscale*, 2013, **5**, 8625–8633.
5 M. Shao, *Electrocatalysis in Fuel Cells*, Springer, London, 2013.
6 X.-H. Yan, G.-R. Zhang and B.-Q. Xu, *Chin. J. Catal.*, 2013, **34**, 1992–1997.
7 X.-H. Yan and B.-Q. Xu, *J. Mater. Chem. A*, 2014, **2**, 8617–8622.
8 M.-Q. Wang, W.-H. Yang, H.-H. Wang, C. Chen, Z.-Y. Zhou and S.-G. Sun, *ACS Catal.*, 2014, **4**, 3928–3936.
9 P. W. Menezes, A. Indra, D. González-Flores, N. R. Sahraie, I. Zaharieva, M. Schwarze, P. Strasser, H. Dau and M. Driess, *ACS Catal.*, 2015, **5**, 2017–2027.
10 G. Wu, K. L. More, C. M. Johnston and P. Zelenay, *Science*, 2011, **332**, 443–447.
11 Y. Liang, Y. Li, H. Wang, J. Zhou, J. Wang, T. Regier and H. Dai, *Nat. Mater.*, 2011, **10**, 780–786.
12 Y. Liang, H. Wang, J. Zhou, Y. Li, J. Wang, T. Regier and H. Dai, *J. Am. Chem. Soc.*, 2012, **134**, 3517–3523.
13 Y. Hu, J. O. Jensen, W. Zhang, L. N. Cleemann, W. Xing, N. J. Bjerrum and Q. Li, *Angew. Chem., Int. Ed.*, 2014, **53**, 3675–3679.
14 H. T. Chung, J. H. Won and P. Zelenay, *Nat. Commun.*, 2013, **4**, 1922.
15 Y. Hou, T. Huang, Z. Wen, S. Mao, S. Cui and J. Chen, *Adv. Energy Mater.*, 2014, **4**, 1400337.
16 M. P. Fernández-García, P. Gorria, M. Sevilla, M. P. Proença, R. Boada, J. Chaboy, A. B. Fuertes and J. A. Blanco, *J. Phys. Chem. C*, 2011, **115**, 5294–5300.
17 G.-X. Zhu, X.-W. Wei and S. Jiang, *J. Mater. Chem.*, 2007, **17**, 2301–2306.
18 Z. Wen, S. Ci, F. Zhang, X. Feng, S. Cui, S. Mao, S. Luo, Z. He and J. Chen, *Adv. Mater.*, 2012, **24**, 1399–1404.
19 J. Deng, P. Ren, D. Deng, L. Yu, F. Yang and X. Bao, *Energy Environ. Sci.*, 2014, **7**, 1919–1923.
20 J. Deng, L. Yu, D. Deng, X. Chen, F. Yang and X. Bao, *J. Mater. Chem. A*, 2013, **1**, 14868–14873.
21 J. Deng, P. Ren, D. Deng and X. Bao, *Angew. Chem., Int. Ed.*, 2015, **54**, 2100–2104.
22 S. H. Noh, D. H. Kwak, M. H. Seo, T. Ohsaka and B. Han, *Electrochim. Acta*, 2014, **140**, 225–231.
23 T. C. Chen, M. Q. Zhao, Q. Zhang, G. L. Tian, J. Q. Huang and F. Wei, *Adv. Funct. Mater.*, 2013, **23**, 5066–5073.
24 D. Deng, L. Yu, X. Chen, G. Wang, L. Jin, X. Pan, J. Deng, G. Sun and X. Bao, *Angew. Chem., Int. Ed.*, 2013, **52**, 371–375.
25 J. Xiao, Q. Kuang, S. Yang, F. Xiao, S. Wang and L. Guo, *Sci. Rep.*, 2013, **3**, 2300–2307.
26 K. Latham, G. Jambu, S. Joseph and S. Donne, *ACS Sustainable Chem. Eng.*, 2014, **2**, 755–764.
27 L. Qu, Y. Liu, J.-B. Baek and L. Dai, *ACS Nano*, 2010, **4**, 1321–1326.
28 D. Kwak, A. Khetan, S. Noh, H. Pitsch and B. Han, *ChemCatChem*, 2014, **6**, 2662–2670.
29 J. K. Nørskov, J. Rossmeisl, A. Logadottir, L. Lindqvist, J. R. Kitchin, T. Bligaard and H. Jonsson, *J. Phys. Chem. B*, 2004, **108**, 17886–17892.
30 B. Hammer and J. K. Nørskov, *Adv. Catal.*, 2000, **45**, 71–129.

